Available online at www.sciencedirect.com
SCIENCE DIRECT®
ELSEVIER
Colloids and Surfaces A: Physicochem. Eng. Aspects 278 (2006) 53–59
COLLOIDS AND SURFACES A
www.elsevier.com/locate/colsurfa

# Effect of hydrophilic group on water droplet contact angles on surfaces of acid modified SiLK and Parylene polymers

S. Pimanpang*, Pei-I Wang, J.J. Senkevich, G.-C. Wang, T.-M. Lu

*Center for Integrated Electronics, Department of Physics, Applied Physics, and Astronomy, Rensselaer Polytechnic Institute, Troy, NY 12180-3590, USA*

Received 3 May 2005; received in revised form 14 November 2005; accepted 29 November 2005
Available online 18 January 2006

**Abstract**

The effect of surface roughness and surface chemistry of SiLK and Parylene polymers on the water droplet contact angle was investigated using Atomic Force Microscopy (AFM) and X-ray Photoelectron Spectroscopy (XPS). AFM images show that the surface morphologies of SiLK and Parylene treated with $H_2SO_4$ and $H_3PO_4$ solutions are qualitatively the same as those of the untreated SiLK and Parylene. However, the advancing ($\theta_a$) and receding ($\theta_r$) contact angles on SiLK dramatically decrease from $\theta_a = 70 \pm 3^\circ$ and $\theta_r = 63 \pm 2^\circ$ to $\theta_a = 37 \pm 2^\circ$ and $\theta_r = 34 \pm 3^\circ$, respectively, after being treated with a $H_2SO_4$ solution. In contrast, the advancing and receding contact angles on SiLK treated with $H_3PO_4$ solution or Parylene treated with $H_2SO_4$ or $H_3PO_4$ solutions were changed within a few degrees. XPS results show that polar functional groups (C=O and –OH) formed on the SiLK sample surface after being treated with $H_2SO_4$ solution. However, $H_3PO_4$ reacts less aggressively with the ethynyl (–C≡C–) bonding on the SiLK surface compared with $H_2SO_4$. Parylene lacks ethynyl chemistry and is therefore chemically more inert than SiLK. Thus, both $H_2SO_4$ and $H_3PO_4$ solutions have fewer reactions with Parylene resulting in slight changes in the advancing and receding contact angles.
© 2005 Elsevier B.V. All rights reserved.

*Keywords:* SiLK; Parylene; Advancing and receding contact angle; X-ray Photoelectron Spectroscopy; Atomic Force Microscopy

## 1. Introduction

SiLK and Parylene-N (PPX) are low-k polymers and have attracted attention for their potential applications in the microelectronics industry. SiLK has many good properties including low dielectric constant (2.65), high thermal stability (>425 °C), and low moisture uptake of 0.24 wt.% at 20 °C and 80% relative humidity (RH) [1], which makes it a good candidate to replace $SiO_2$ for Cu interconnect technology. PPX also has a low dielectric constant of 2.66 [1], and moreover, it is highly chemically inert so it also has applications in moisture barrier and chemical and corrosion resistance coatings.

SiLK and PPX polymers have poor wetting and adhesion to metals. Many research groups have proposed various approaches to improve the wetting and adhesion properties of polymers such as $Ag^-$ ion implantation (to avoid charging problems on insulator surfaces) [2], $O_2/NF_3$, $O_2$, remote argon, $N_2$ plasma [3–6], ultraviolet-ozone [6], and $(NH_4)_2S$ solution [7]. The goal of this work is to modify the surface chemistry to improve the wetting and adhesion by creating various functional groups such as –OH group on the polymer surfaces [6,8–10]. However, ion implantations and plasma treatments generally roughen the polymer surfaces and result in more electron scattering and subsequently an increase of metal thin film resistance. The major advantage of improving the polymer wettability and adhesion by acid treatment is that the acid treatments cause less damage to the polymer surface than ion implantations or plasma treatments. The $(NH_4)_2S$ solution has been used to treat Trikon, SiLK, and PPX polymers and the decrease of the water droplet contact angle due to the introduction of hydrophilic groups was observed [7]. In the case of Trikon, this was especially evident, as its advancing contact angle decreased dramatically from ∼100° to below ∼12°. However, the advancing contact angles of $(NH_4)_2S$ treated SiLK and high molecular weight PPX polymers only decreased from ∼78 to ∼64° and from ∼80 to ∼75°, respectively.

The aim of this work is to improve the wettability of SiLK and PPX by functionalizing the polymer surfaces using $H_2SO_4$ and $H_3PO_4$ acid treatments. Here, we present our investigation

* Corresponding author. Tel.: +1 518 253 7681.
*E-mail address:* pimans@rpi.edu (S. Pimanpang).

0927-7757/$ – see front matter © 2005 Elsevier B.V. All rights reserved.
doi:10.1016/j.colsurfa.2005.11.099

of surface morphology and surface chemistry on the acid-treated SiLK and PPX polymers and their corresponding contact angles with de-ionized water (DI-$H_2O$) droplets. The surface morphology was studied using Atomic Force Microscopy (AFM) and the change of surface chemistry was determined using X-ray Photoelectron Spectroscopy (XPS). The results of these investigations show that the wetting of SiLK can be improved by $H_2SO_4$ treatment without significantly affecting its surface morphology. We discussed results and elucidate possible mechanisms and implications.

## 2. Experimental

### 2.1. Sample preparation

Parylene-N (PPX) polymer film was deposited on the Si wafer by chemical vapor deposition (CVD) technique. The PPX reactor consists of a sublimation furnace, a pyrolysis furnace, and a deposition chamber with a bell jar. The base pressure in the deposition chamber was at mid $10^{-6}$ Torr and during deposition the chamber pressure was 2 mTorr. A detailed description of the reactor and deposition process has been presented elsewhere [11,12]. Briefly, the precursor [2,2]paracyclophane was sublimed at a temperature of 155 °C, and transported to a high temperature region (650 °C) of the reactor inlet where most precursors was cleaved into two *p*-xylylene monomers by vapor phase pyrolysis. These reactive intermediate *p*-xylylene monomers were then transported to a room temperature deposition chamber where physisorption and subsequent polymerization took place. Linear chains of poly(*p*-xylylene) or PPX were formed. SiLK polymer film was deposited on a Si wafer by a spin coating technique, and the SiLK polymer film was provided by IBM. The polymer films were dipped into a sulfuric ($H_2SO_4$) of 50 vol% at room-temperature or the phosphoric ($H_3PO_4$) of 85 vol% at 80 °C for 30 s and then rinsed in the de-ionized (DI) water for 30 s and followed by nitrogen gas blow-drying [13]. The as-deposited and acid-treated polymer film thickness was determined using a Variable Angle Spectroscopic Ellipsometer (M-44, J.A. Woollam Co., Lincoln, Nebraska). No detectable changes of the film thickness after the acid treatments were observed.

### 2.2. Contact angle

The sessile drop technique was used to measure the contact angle where a 5 μL drop of distilled water in a syringe was dropped on the sample surface at room temperature. The water droplet formed an equilibrium dome shape on the horizontal sample surface and imaged by a microscope (Intel Play QX3) with a 60× magnification. The advancing ($\theta_a$) and receding ($\theta_r$) contact angles were measured by the tilting-plate goniometric technique. The sample was slowly tilted in 5° increments from the horizontal position and the water droplet was imaged with a microscope in order to observe any changes to the droplet contact angle on both the left and right sides of the droplet. The maximum $\theta_a$ and minimum $\theta_r$ were attained when the droplet was at the incipient motion [14]. However, finding the incipient point is not convenient experimentally so the common procedure is to plot the observed contact angle (either to obtain $\theta_a$ or $\theta_r$) versus the tilting angle. For each of these plots, either $\theta_a$ or $\theta_r$ is obtained by the average of the points on this plot where the observed contact angle stabilizes.

### 2.3. AFM and XPS

The surface morphologies after acid treatments were imaged and analyzed using Atomic Force Microscopy (AFM) and the associated image software (Park Scientific Instrument). Surface images were scanned in non-contact mode at four different locations on each sample to detect any difference in surface morphology. The surface chemical bonding on each sample was analyzed using X-ray Photoelectron Spectroscopy (XPS). The samples were loaded into a stainless chamber with a base pressure of (∼1 to 2) × $10^{-9}$ Torr. During the collection of an XPS spectrum the pressure rose to (∼3 to 4) × $10^{-9}$ Torr. The X-ray Mg Kα source (PHI model 04-151) used in this experiment had a primary energy of 1253.6 eV, and a double pass cylindrical mirror energy analyzer controller (PHI Model 15-255G) was used to detect the electrons. A high-resolution spectrum averaged over 40 repeated scans was collected at a passing energy of 50 eV.

## 3. Results and discussion

Fig. 1 shows the images of the water droplets on untreated and $H_2SO_4$ solution treated SiLK and PPX samples in the horizontal position. Their advancing and receding contact angles were analyzed by the tilting-plate goniometric technique and the angles are listed in Table 1. We observed a significant decrease of the advancing and receding contact angles of the water droplets from $\theta_a = 70 \pm 3°$ and $\theta_r = 63 \pm 2°$ to $\theta_a = 37 \pm 2°$ and $\theta_r = 34 \pm 3°$, respectively, on SiLK treated with the $H_2SO_4$ solution. However, the contact angles of SiLK treated with the $H_3PO_4$ solution and PPX treated with either $H_2SO_4$ or $H_3PO_4$ solution showed only slight changes.

The wetting of material surfaces generally depends on two major factors: chemical functionality and/or surface roughness [15]. Changes in either chemical or surface morphology will contribute to the observed value of the contact angle. By treating SiLK and PPX surfaces with either $H_2SO_4$ or $H_3PO_4$ solution, both the surface chemistry and surface morphology may be modified and result in contact angle changes.

### 3.1. Surface morphology

The effect of surface roughness on the liquid droplet contact angle has been studied both theoretically and experimentally [16–23]. Wenzel first predicted that a change in surface roughness will affect the liquid droplet contact angle [16] and gave the relationship between a contact angle and the roughness area ratio as

$$\cos\theta_R = W_R \cos\theta_o, \quad (1)$$

where $W_R$ is the roughness area ratio (true area/nominal area), $\theta_R$ and $\theta_o$ are the contact angles of water drops on rough surface and

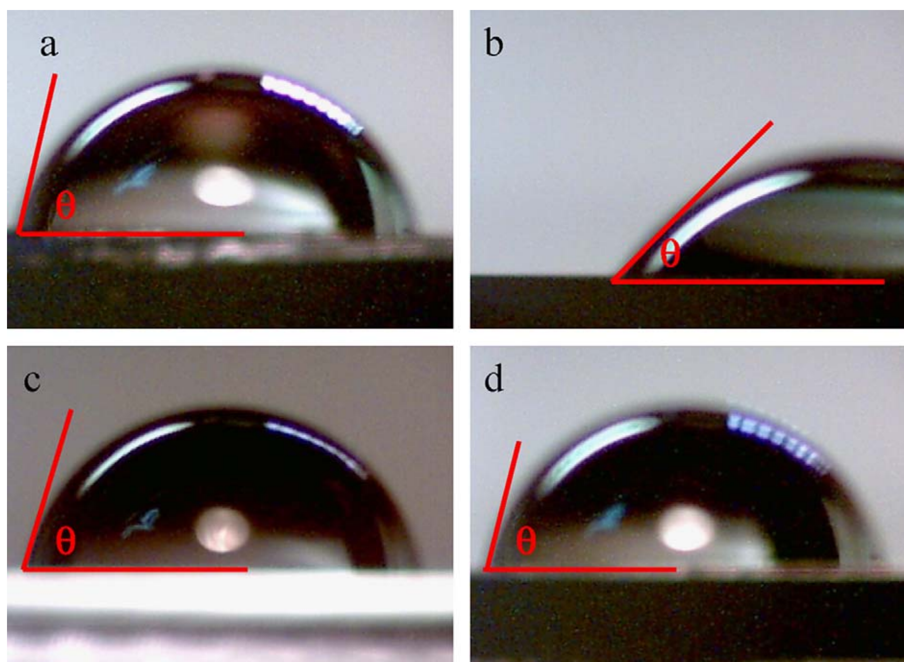


Fig. 1. The images and contact angles of water droplets on sample surfaces positioned horizontally before tilting of the samples. The images were taken by a microscope with a 60× magnification. (a) Untreated SiLK, 70 ± 3°, (b) SiLK treated with $H_2SO_4$ solution (half of the water droplet spreads beyond the camera's viewing field), 37 ± 2°, (c) untreated Parylene, 76 ± 2°, and (d) Parylene treated with $H_2SO_4$ solution, 70 ± 2°.

smooth surface, respectively. From Wenzel's Eq. (1), the surface must become very rough in order to increase the true surface area, which will then increase $W_R$ and results in a significant change on the liquid droplet contact angle. In order to detect the change on surface roughness and $W_R$ on SiLK and PPX surfaces after the acid treatments, Atomic Force Microscopy (AFM) was used to image and analyze these polymer surface morphologies.

The 4 μm × 4 μm 3D AFM images in Fig. 2a and b show the surface morphology of untreated SiLK and SiLK after being treated with $H_2SO_4$ solution, respectively. These two images qualitatively have a similar surface roughness. Table 1 lists the vertical root mean square roughness ($w$) of the untreated SiLK, SiLK treated with $H_3PO_4$ acid, and SiLK treated with $H_2SO_4$ acid obtained from the AFM results to be about 0.440, 0.468, and 0.443 nm, respectively. The small change of $w$ after either $H_2SO_4$ acid treatment or $H_3PO_4$ acid treatment suggests that SiLK surface undergoes a very small change after the acid treatments.

Table 1
The measured advancing ($\theta_a$) and receding ($\theta_r$) contact angles, and the values of vertical root mean square roughness ($w$) analyzed from the AFM images for untreated and acid ($H_3PO_4$ or $H_2SO_4$) treated SiLK and Parylene (PPX) polymers

| Sample | $\theta_a$ (°) | $\theta_r$ (°) | $w$ (nm) |
|---|---|---|---|
| Untreated SiLK | 70 ± 3 | 63 ± 2 | 0.440 |
| $H_3PO_4$ treated SiLK | 76 ± 3 | 71 ± 3 | 0.468 |
| $H_2SO_4$ treated SiLK | 37 ± 2 | 34 ± 3 | 0.443 |
| Untreated PPX | 76 ± 2 | 65 ± 3 | 3.502 |
| $H_3PO_4$ treated PPX | 78 ± 4 | 70 ± 3 | 3.058 |
| $H_2SO_4$ treated PPX | 70 ± 2 | 64 ± 3 | 3.269 |

Similarly, the surface morphology of the acid treated PPX shows a nominal change after treated with either $H_3PO_4$ or $H_2SO_4$ acid compared to that of the untreated PPX. The 4 μm × 4 μm 3D AFM image of the untreated PPX surface morphology (Fig. 2c) shows a similar surface morphology as that of the $H_2SO_4$ acid treated PPX (Fig. 2d), which suggests that $H_2SO_4$ acid treatment has a small effect on the PPX surface morphology. Table 1 lists the root mean square roughness ($w$) of the untreated PPX, PPX treated with $H_3PO_4$ acid, and PPX treated with $H_2SO_4$ acid to be about 3.502, 3.058, and 3.269 nm, respectively.

The AFM result shows that SiLK and PPX surfaces undergo a nominal change after either treated with $H_2SO_4$ solution or $H_3PO_4$ solution, thus, the water droplet contact angle should not have a significant change for all cases. However, the advancing and receding contact angle decrease significantly in case of SiLK treated with $H_2SO_4$ solution even though the surface morphology change of SiLK treated with $H_2SO_4$ solution is in a nanometer scale. Therefore, the surface morphology change of SiLK treated with $H_2SO_4$ solution should not be the main contributor to the significant decrease of the advancing and receding water droplet contact angles. This observation leads to a hypothesis that any change of surface chemistry on SiLK treated with $H_2SO_4$ acid solution may play a more dominant role in the decrease of the water droplet contact angle.

### 3.2. Surface chemistry

XPS analyses were performed from spectra collected from both SiLK and PPX treated with either $H_2SO_4$ or $H_3PO_4$ solution. Neither sulfur nor phosphorus peaks were observed on the polymer after acid treatments. In contrast, polar functional

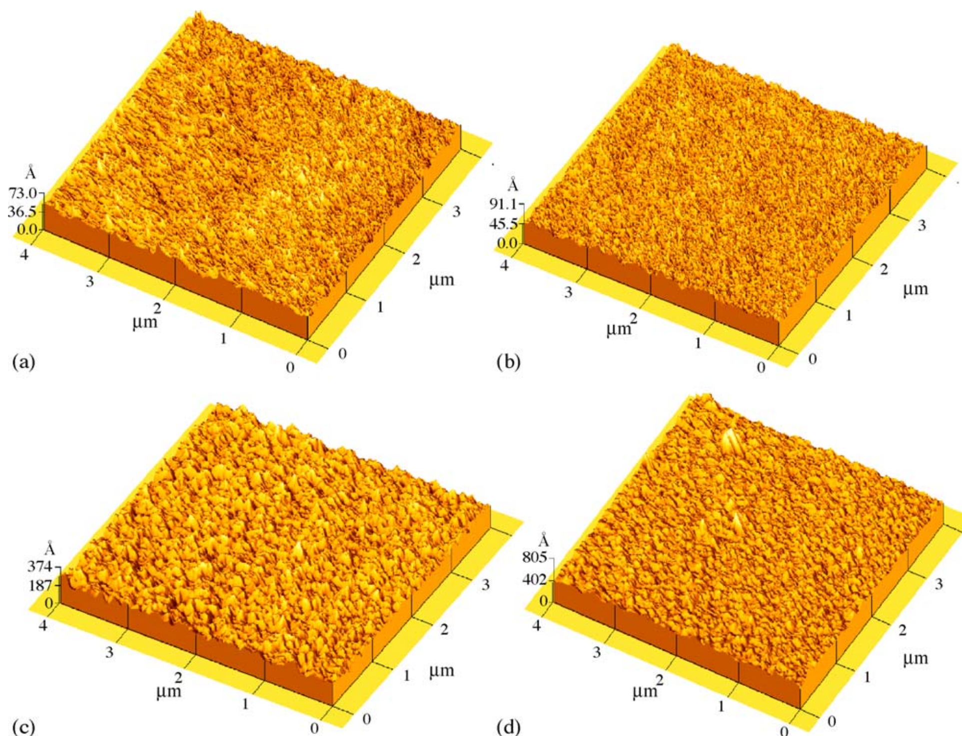


Fig. 2. The 4 μm × 4 μm 3D AFM images of (a) untreated SiLK with rms roughness $w = 0.440$ nm, (b) SiLK treated with $H_2SO_4$ solution with $w = 0.443$ nm, (c) untreated PPX with $w = 3.502$ nm, and (d) Parylene treated with $H_2SO_4$ solution with $w = 3.269$ nm.

groups composed of C–OH and C=O were incorporated onto the SiLK surface after being treated with $H_2SO_4$. The change of the surface chemistry or the presence of the polar functional groups on the polymer surface will change the apparent contact angle because different surface chemistries have different surface energies [2,5,7,24].

Fig. 3a shows that the C 1s core level spectrum of untreated SiLK surface can be decomposed into two peaks: C–H bonding and C–O bonding at 284.6 and 286.2 eV, respectively. The C–H bonding at binding energy 284.6 eV was used as the reference. This result agrees with the untreated sample obtained by Yu et al. [25,26]. The C 1s spectrum of SiLK treated with the $H_3PO_4$ solution is still composed of these two peaks (not shown in Fig. 3a). The ratio of integrated peak areas C–H/C–O is very close to that of untreated SiLK as listed in Table 2, suggesting that SiLK is not reactive with the $H_3PO_4$ solution. However, in the case of SiLK treated with $H_2SO_4$ solution, the change of the C 1s spectrum is more visible. The best curve fit for C 1s spectrum of SiLK treated with the $H_2SO_4$ solution consists of three different species: C–H bonding, C–O bonding, and C=O bonding, where C=O binging energy is at 287.5 eV, which are shown in Fig. 3a. The results of the areas obtained from curve fits for SiLK untreated, SiLK treated with $H_3PO_4$, and $H_2SO_4$ solutions are summarized in Table 2. The ratio of the integrated peak area C–H/C–O of SiLK treated with $H_2SO_4$ solution is significantly lower (∼7) than those of untreated SiLK (∼16) and SiLK treated with $H_3PO_4$ solution (∼18).

The decrease in the ratio of the integrated XPS peak area C–H/C–O and the existence of C=O at the SiLK surface after being treated with $H_2SO_4$ solution suggests that certain bonds of SiLK react with $H_2SO_4$ solution. This chemical reaction facil-

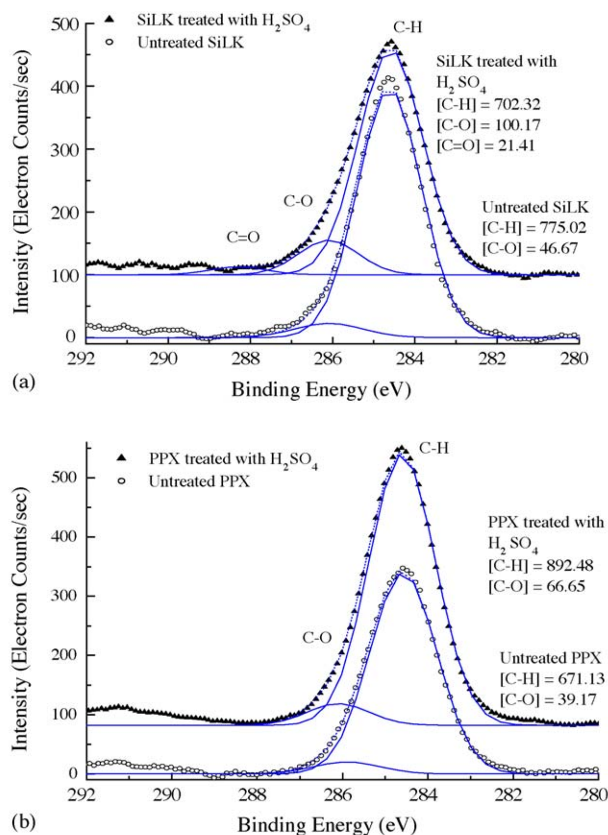


Fig. 3. XPS C 1s spectra of (a) SiLK untreated and SiLK treated with the $H_2SO_4$ solution and (b) PPX untreated and treated with $H_2SO_4$ solution. The peak fit gives peaks C—H, C—O and C=O. The number to the right hand side of the equal sign is the integrated intensity area from a peak fit.

Table 2
The areas of integrated XPS intensity for C—H, C—O, C=O peaks and ratio of areas C—H/C—O of C 1s spectra for untreated and acid ($H_3PO_4$ or $H_2SO_4$) treated SiLK and Parylene (PPX) polymer samples

| Sample | Area of C—H (a.u.) | Area of C—O (a.u.) | Area of C=O (a.u.) | Area ratio of C—H/C—O |
|---|---|---|---|---|
| Untreated SiLK | 775.02 | 46.67 | – | 16.61 |
| $H_3PO_4$ treated SiLK | 817.93 | 45.34 | – | 18.04 |
| $H_2SO_4$ treated SiLK | 702.32 | 100.17 | 21.41 | 7.01 |
| Untreated PPX | 671.13 | 39.17 | – | 17.13 |
| $H_3PO_4$ treated PPX | 744.54 | 54.45 | – | 13.67 |
| $H_2SO_4$ treated PPX | 892.48 | 66.62 | – | 13.40 |

itates the formation of polar functional groups (C=O or –OH) on the polymer surface. A similar phenomenon has also been observed by Yu et al. [25,26] with SiLK treated by Ar plasma and subsequently exposed to air. Ar plasma is able to break chemical bonds and introduces free radicals on SiLK surface. These free radicals facilitate the formation of polar functional groups (–OOH and –O–O–) during the exposure to air. However, the strong Ar plasma energy not only modifies the SiLK surface chemistry, but also roughens the SiLK surface. On the contrary, the $H_2SO_4$ solution seems to only break and/or react with certain unsaturated bonds in the chemical structure of SiLK. The formation of SiLK cross-link has been reported and discussed [1]. Fig. 4a shows that the SiLK cross-link contains the ethynyl bonding (–C≡C–) that has a much higher reactivity than aliphatic bonding (–C–C–) [27]. Thus, we believe that the reaction of SiLK with $H_2SO_4$ solution should take place at the SiLK cross-link, and carries out in the following mechanism:

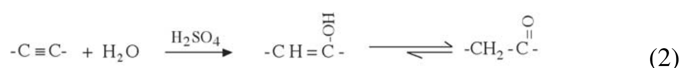


(2)

The mechanism shown in Eq. (2) is supported by the increase of the integrated area of the XPS peak associated with the C–O bond and the appearance of C=O in the C 1s spectrum of SiLK after $H_2SO_4$ treatment, see Fig. 3a. However, the $H_3PO_4$ is less acidic than $H_2SO_4$ and has difficulty reacting with the –C≡C– bonds. The C 1s peak of SiLK treated with $H_2SO_4$ solution (Fig. 3a) shows that the integrated area of C–O is higher than the integrated area of C=O even though the C–OH bonding can become the C=O bonding easier than the C=O bonding converting back to the C–OH bonding as indicated by the long and short arrows, respectively in Eq. (6). We are not clear about the reason

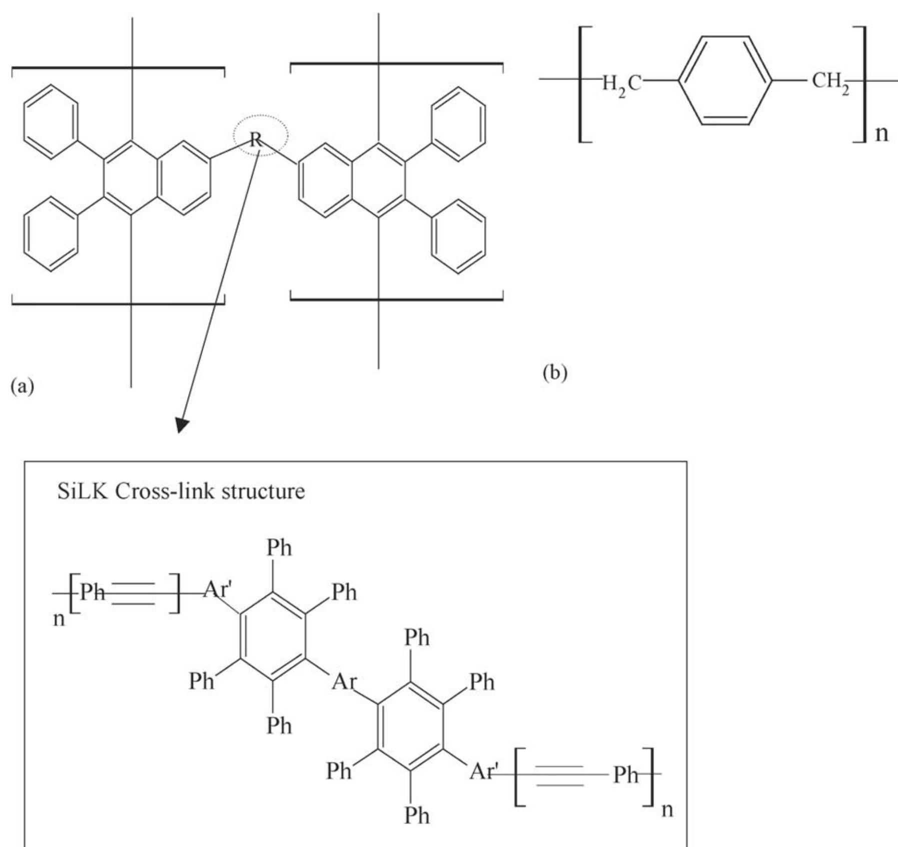


Fig. 4. The chemical structures of (a) SiLK and part of SiLK cross-link and (b) the PPX polymer. Where O, Ph and Ar are oxygen, phenyl, and aromatic ring, respectively.

why we observed a higher C–O bonding than a C=O bonding. However, the significant decrease of the advancing and receding contact angles on SiLK after being treated with $H_2SO_4$ solution agrees with the observation of a higher C–O bonding than a C=O bonding. This is because the C–OH bonding can form a strong hydrogen bond with the water molecules but the C=O bonding cannot form the hydrogen bond with the water molecules. Other possible causes of the change of the water droplet contact angle may due to the SiLK chain reorientation during the acid treatment or during the contact angle measurement and the penetration of the liquid into the polymer.

It has been reported that the free radicals (chain ends) of PPX are very reactive with oxygen in the air and form the peroxy group (–*O*–*O*•) [7]. Similarly, the peroxy groups would also form on the available SiLK free radicals on the SiLK surface in an oxygen-containing environment. The peroxy group on polymer surface is unstable and tends to be replaced by –OH or =O groups when being dipped into an acid solution. The small number of polar groups formed at chain ends of free radicals on the $H_3PO_4$ treated SiLK surface slightly changes the SiLK surface energy resulting in a small change of the water droplet contact angle. The small amount of polar function groups formed on the SiLK treated with $H_3PO_4$ solution at the free radicals causes the ratio of integrated XPS peak area C–H/C–O of SiLK treated with $H_3PO_4$ solution (∼18.04) to be slightly different from that of untreated SiLK (∼16.61).

Fig. 5 illustrates a mechanism of the formation of polar functional groups on SiLK surface after treated with $H_2SO_4$ solution. In conjunction with the above AFM result, it appears that the $H_2SO_4$ solution introduces a significant change in the SiLK surface chemistry by forming polar functional groups composed of –OH and =O on the surface, which is the major factor responsible for the dramatic decrease of the advancing and receding contact angles, while $H_2SO_4$ treatment has only a minor effect to the SiLK surface morphology.

Fig. 3b shows that the C 1s spectrum of untreated PPX. It is composed of two species: C–H bonding and C–O bonding with binding energies of 284.6 and 286.2 eV, respectively. No significant change is observed in the XPS spectra of PPX treated with either $H_2SO_4$ or $H_3PO_4$ solutions. The ratios of integrated XPS peak areas C–H/C–O of PPX treated with either $H_2SO_4$ or $H_3PO_4$ solutions listed in Table 2 are similar to the ratio for untreated PPX. It appears that both $H_2SO_4$ and $H_3PO_4$ solutions are not acidic enough to react with aliphatic bonds (–C–C–) in the PPX polymer chain (Fig. 4b). Therefore, the formation of polar groups on the PPX surface merely relies on the chemical reaction on PPX free radicals and leads to only a slight change of the advancing and receding contact angles. This result further supports our proposed chemical reaction mechanism that $H_2SO_4$ solution can only react with the ethynyl chemistry in SiLK while it is not aggressive enough to react with the carbon-carbon single bond in Parylene. The small amount of polar function groups formed at the free radicals on the PPX after treated with $H_2SO_4$ or $H_3PO_4$ solutions causes the ratio of integrated XPS peak areas C–H/C–O of PPX treated with $H_2SO_4$ or $H_3PO_4$ solutions differs slightly from that of untreated PPX as listed in Table 2. The small amount of polar functional groups formed on PPX at free radicals after the acid treatments results in the slight change of the water droplet contact angle. Other possible causes of contact angle change may include the PPX chain reorientation or the liquid penetration into the polymer.

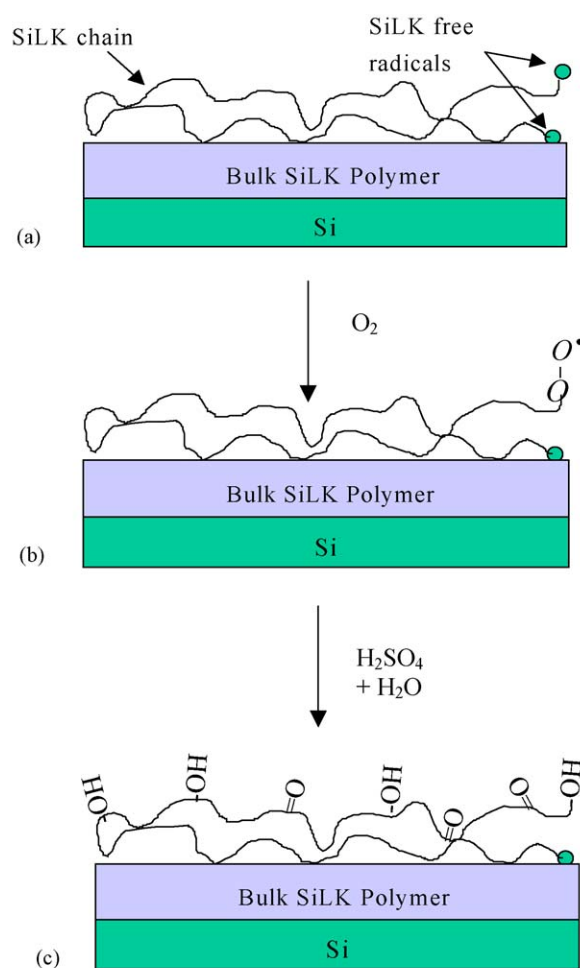


Fig. 5. A proposed mechanism of the formation of polar functional groups on SiLK surface after reacting with $H_2SO_4$ solution. (a) Unexposed SiLK chains and SiLK free radicals to the air. The shaded filled circles represent SiLK free radicals. (b) Peroxy (–*O*—*O*•) formed at the free radicals when exposed in the air that contains $O_2$. (c) The –C≡C– bond on SiLK cross-links at the surface reacts with $H_2SO_4$ solution and forms polar function groups C=O and –OH.

## 4. Conclusion

Our results of AFM and XPS support that a dramatic decrease in the advancing and receding contact angles on SiLK treated with $H_2SO_4$ solution is attributed to the increase of polar functional groups (C=O and –OH) on SiLK surface instead of the change on surface morphology. The $H_2SO_4$ solution tends to react with the ethynyl bonding at the SiLK surface. The polar functional groups are introduced on SiLK surface after $H_2SO_4$ treatment and it decreases the advancing and receding contact angles from $\theta_a = 70 \pm 3°$ and $\theta_r = 63 \pm 2°$ to $\theta_a = 37 \pm 2°$ and $\theta_r = 34 \pm 3°$, respectively. $H_3PO_4$ solution is not aggressive enough to react with any SiLK bond so there are no polar groups present at the SiLK surface. Parylene is more chemically inert than the SiLK polymer so that both $H_2SO_4$ and $H_3PO_4$

solutions cannot react with its aliphatic bonding. That the slight changes of the advancing and receding contact angles on SiLK treated with the $H_3PO_4$ solution and PPX treated with either $H_2SO_4$ or $H_3PO_4$ solutions is attributed to a small amount of polar functional groups created by the chemical reaction of the acid solutions with the unstable free radicals on SiLK and PPX polymer surfaces.

## Acknowledgments

We thank A. Kumar for suggestions and B. Carrow for valuable discussions. Samuk Pimanpang thanks the Thai government for a fellowship.

## References

[1] S.J. Martin, J.P. Godschalx, M.E. Mills, E.O. Shaffer II, P.H. Townsend, Adv. Mater. 12 (2000) 1769.
[2] Hiroshi Tsuji, Hiroko Satoh, Shigeki Ikeda, Yasuhito Gotoh, Junzo Ishikawa, Nuclear Instrum. Methods Phys. Res. B 141 (1998) 197.
[3] M.R. Baklanov, S. Vanhaelemeersch, H. Bender, K. Maex, J. Vac. Sci. Technol. B 17 (1999) 372.
[4] D.M. Choi, C.K. Park, K. Cho, C.E. Park, Polymer 38 (1997) 6243.
[5] B. Gupta, J. Hilborn, Ch. Hollenstein, C.J.G. Plummer, R. Houriet, N. Xanthopolus, J. Appl. Polym. Sci. 78 (2000) 1083.
[6] B.W. Callen, M.L. Ridge, S. Lahooti, A.W. Neumann, R.N.S. Sodhi, J. Vac. Sci. Technol. A 13 (1995) 2023.
[7] Jay J. Senkevich, G.R. Yang, T.-M. Lu, Colloids. Surf. A 214 (2003) 119.
[8] Jay J. Senkevich, Boquan Li, G.-R. Yang, G.-C. Wang, T.-M. Lu, Electrochem. Solid-State Lett. 5 (2002) C94.
[9] Minghui Hu, Suguru Noda, Yoshiko Tsuji, Tatsuya Okubo, Yukio Yamaguchi, Hiroshi Komiyama, J. Vac. Sci. Technol. A 20 (2002) 589.
[10] G.C. Herdt, A.W. Czanderna, J. Vac. Sci. Technol. A 17 (1999) 3415.
[11] J.B. Fortin, T.-M. Lu, J. Vac. Sci. Technol. A 18 (5) (2000) 2459.
[12] J.B. Fortin, T.-M. Lu, Chem. Mater. 14 (2002) 1945.
[13] Pei-I Wang, T.-M. Lu, S.P. Murarka, R. Ghoshal, US Patent Pending “Chemical treatment of material surfaces”.
[14] I.D. Morrison, S. Ross, Colloidal Dispersions: Suspensions, Emulsions and Foams, John Wiley and Sons, 2002, p. 226.
[15] N. Eustathopolos, M.G. Nicholas, B. Drevet, Wettability at High Temperatures, Pergamon, 1999, p. 22.
[16] R.N. Wenzel, Ind. Eng. Chem. 28 (1936) 988.
[17] J.F. Oliver, S.G. Mason, J. Mater. Sci. 15 (1980) 431.
[18] J.F. Oliver, C. Huh, S.G. Mason, J. Adhesion 8 (1977) 223.
[19] S.J. Hitchcock, N.T. Carroll, M.G. Nicholas, J. Mater. Sci. 16 (1981) 714.
[20] Gershon Wolansky, Abraham Marmur, Colloids Surf. A 156 (1999) 381.
[21] B. Muller, M. Riedel, R. Michel, S.M. De Paul, R. Hofer, D. Heger, D. Grutzmacher, J. Vac. Sci. Technol. A 19 (2001) 1715.
[22] H. Nakae, R. Inui, Y. Hirata, H. Saito, Acta Mater. 46 (1998) 2313.
[23] Y.-Y. Chen, J.-G. Duh, B.-S. Chiou, J. Mater. Sci.: Mater. Electron. 11 (2000) 279.
[24] Ron S. Faibish, Wayne Yoshida, Yoram Cohen, J. Colloid Interface Sci. 256 (2002) 341.
[25] W.H. Yu, Y. Zhang, E.T. Kang, K.G. Neoh, S.Y. Wu, Y.F. Chow, J. Electrochem. Soc. 149 (2002) C521.
[26] W.H. Yu, Y. Zhang, E.T. Kang, K.G. Neoh, S.Y. Wu, Y.F. Chow, J. Electrochem. Soc. 150 (2003) F156.
[27] Rodger W. Griffin Jr., Modern Organic Chemistry, McGraw-Hill Book Company, 1969, p. 100.